Unconstrained detection of respiration rhythm and pulse rate with one under-pillow sensor during sleep

W. Chen[1] X. Zhu[2] T. Nemoto[3] Y. Kanemitsu[4] K. Kitamura[3] K. Yamakoshi[5]

[1]Department of Computer Software, University of Aizu, Aizu-wakamatsu City, Japan
[2]Graduate Department of Information Systems, University of Aizu, Aizu-wakamatsu City, Japan
[3]Faculty of Medicine, Kanazawa University, Kanazawa City, Japan
[4]SRI Research & Development Ltd, Kobe City, Japan
[5]Faculty of Engineering, Kanazawa University, Kanazawa City, Japan

Abstract—*A completely non-invasive and unconstrained method is proposed to detect respiration rhythm and pulse rate during sleep. By employing wavelet transformation (WT), waveforms corresponding to the respiration rhythm and pulse rate can be extracted from a pulsatile pressure signal acquired by a pressure sensor under a pillow. The respiration rhythm was obtained by an upward zero-crossing point detection algorithm from the respiration-related waveform reconstructed from the WT 2^6 scale approximation, and the pulse rate was estimated by a peak point detection algorithm from the pulse-related waveform reconstructed from the WT 2^4 and 2^5 scale details. The finger photo-electric plethysmogram (FPP) and nasal thermistor signals were recorded simultaneously as reference signals. The reference pulse rate and respiration rhythm were detected with the peak and upward zero-crossing point detection algorithm. This method was verified using about 24 h of data collected from 13 healthy subjects. The results showed that, compared with the reference data, the average error rates were 3.03% false negative and 1.47% false positive for pulse rate detection in the extracted pulse waveform. Similarly, 4.58% false negative and 3.07% false positive were obtained for respiration rhythm detection in the extracted respiration waveform. This study suggests that the proposed method is suitable, in sleep monitoring, for the diagnosis of sleep apnoea or sudden death syndrome.*

Keywords—*Respiration rhythm, Pulse rate, Wavelet transformation, Sleep, Unconstrained monitor*

Med. Biol. Eng. Comput., 2005, **43**, 306–312

1 Introduction

MONITORING OF both respiration rhythm and heart rate plays an important role in the diagnosis of sleep apnoea and sudden death syndrome. There are numerous traditional methods in respiration measurement, such as the use of spirometers, nasal thermocouples, body volume changes, transthoracic inductances, impedance plethysmographs, strain gauge measurements of thoracic circumference, pneumatic respiration transducers, whole-body plethysmographs and ECG-based derived respiration (MOODY *et al.*, 1985). However, all these methods can cause discomfort and inconvenience to the subject and physician, because the sensor must be put on the body surface. Heart rate monitoring based on vital signs, such as the ECG, heart sound and finger photo-electric plethysmogram (FPP), also requires appropriate sensors to be placed on the subject.

NAKAJIMA *et al.* (2001; 2002) developed a low-cost, pillow-shaped respiratory monitor to meet the requirement for non-invasive and unconstrained measurement. WATANABE *et al.* (2003) devised a new instrument to obtain the respiration rhythm and pulse rate from pulsatile pressure signals acquired from two water-filled cuffs under the head of the subject. As the main signal components in the respiration rhythm (about 10–20 min^{-1}) and pulse rate (about 50–80 min^{-1}) are in different frequency bands, the respiration rhythm was separated with a low-pass filter with a passband of 0.1–0.8 Hz, and the pulse rate was directly estimated from the raw signal with the peak detection method. Apparently, a low-pass filter with such a narrow passbandwidth is hard to design and requires a large computational cost; and the respiration and high-frequency noise in the raw signal will greatly deteriorate the estimation of the pulse rate.

UCHIDA *et al.* (2003) applied independent component analysis (ICA) to separate noise from simultaneously collected

Correspondence should be addressed to Dr Wenxi Chen; email: wenxi@u-aizu.ac.jp, or Mr Xin Zhu; email: d8051101@u-aizu.ac.jp

Paper received 25 May 2004 and in final form 25 October 2004

MBEC online number: 20053983

two-channel signals. However, because the time lag between the two pressure signals does not conform to the instantaneous hypothesis of the ICA linear-mixing model, the respiration rhythm and pulse rate related components cannot be separated well by the classical ICA algorithm. Therefore a revised ICA algorithm may be required to resolve the above problem. On the other hand, spectral analysis should overcome the problem of spectrum crossover among useful signal components, noise and movement artifacts (KANEMITSU *et al.*, 2004).

Wavelet transformation (WT) (MALLAT, 1989; MALLAT and ZHONG, 1992) has found many applications in the biomedical signal-processing field. WT multiresolution analysis can be applied to remove non-white or high-frequency noise (TASWELL, 2000), to detect singularity signals (LI *et al.*, 1995), to perform data compression (HILTON, 1997) and to extract the fetal ECG (KHAMENE and NEGAHDARIPOUR, 2000). In addition, fast WT can be easily realised with either the Mallat (MALLAT, 1989) or *á trous* algorithm (SHENSA, 1992) for real-time signal processing.

2. Methods

2.1 *Measurement system and signals*

A schematic representation of the measurement system is shown in Fig. 1. Two under-pillow incompressible tubes, 30 cm in length and 2 cm in diameter, were filled with air-free water, with preloaded internal pressure of 3 kPa, and embedded with an arterial catheter 15 cm long in one end of each tube. These two tubes were set in parallel under the near-neck occiput and the far-neck occiput, at a distance of 13 cm from each other. Both the static and dynamic components of the pressure within the tubes were measured by pressure amplifiers* connected to the embedded catheters. The static pressure component corresponded to the weight of the head, and the dynamic component reflected the weight fluctuation of the head caused by breathing movements and pulsatile blood flow from the external carotid arteries around the head. After filtering with an analogue filter with a pass-band of 0.16–5 Hz, filtered pressure signals were digitised onto a PC through a 16-bit analogue-to-digital (AD) converter board and stored for batch analysis.

The pillow was stuffed with numerous fragments of soft material made of synthetic resins for comfort. Signals could be collected non-invasively and unconstrainedly while the subject was sleeping in a supine or recumbent position. FPP and nasal thermistor measurements were saved together as reference data. The sampling rate was 100 Hz for all four signals.

Fig. 2 shows typical measured signals. The upper two rows display pulsatile pressure waveforms in the far-neck occiput (Fig. 2*a*) and the near-neck occiput (Fig. 2*b*). The lower two rows are FPP (Fig. 2*c*) and nasal thermistor (Fig. 2*d*) reference signals, respectively. It can be observed from Figs 2*a* and *b* that the respiration rhythm in the near-neck occiput was later than in the far-neck occiput, where there was nearly no pulse-related waveform. In Figs 2*b* and *c*, pulse waveforms found in the near-neck occiput pressure are almost synchronous with those in the FPP beat-by-beat. Furthermore, the respiration rhythm can be found clearly in both pressure signals (Figs 2*a* and *b*) and the nasal thermistor signal (Fig. 2*d*), although the former seems earlier than the latter. In this paper, only the near-neck occiput pressure signal (Fig. 2*b*) was chosen to detect the respiration rhythm and pulse rate.

*AP-13, Keyence Corp.

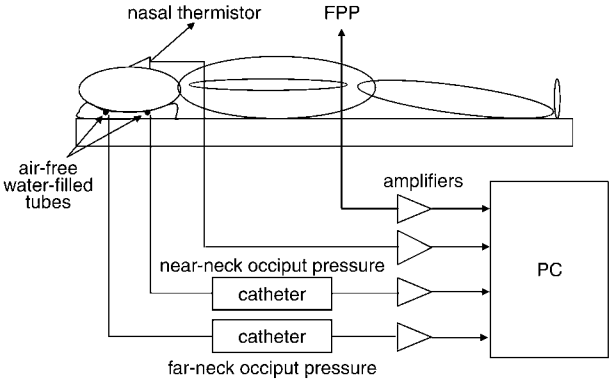

Fig. 1 *Pillow with two air-free water-filled tubes and data acquisition system, including finger photo-electric plethysmogram (FPP) and nasal thermistor signal as references*

2.2 *Principle of wavelet transformation*

WT has become an attractive data analysis tool in the field of biological signal processing. Detailed mathematical theories and algorithms can be found in DAUBECHIES (1992) and AKAY (1998).

The WT of a signal $x(t)$ is defined as follows:

$$W_s x(t) = \frac{1}{s}\int_{-\infty}^{+\infty} x(\tau)\psi(\frac{t-\tau}{s})d\tau \quad (1)$$

where s is the scale factor, and $\psi(t)$ is the wavelet basis function. It is called a dyadic WT if $s = 2^j (j \in Z, Z$ is the integral set) in MALLAT and HWANG (1992). Two filter banks, the low- and high-pass decomposition filters $\boldsymbol{H}_0$ and $\boldsymbol{H}_1$ and associated reconstruction filters $\boldsymbol{G}_0$ and $\boldsymbol{G}_1$, can be derived from the wavelet basis function and its scaling function (MALLAT, 1992). With the Mallat algorithm, the dyadic WT of

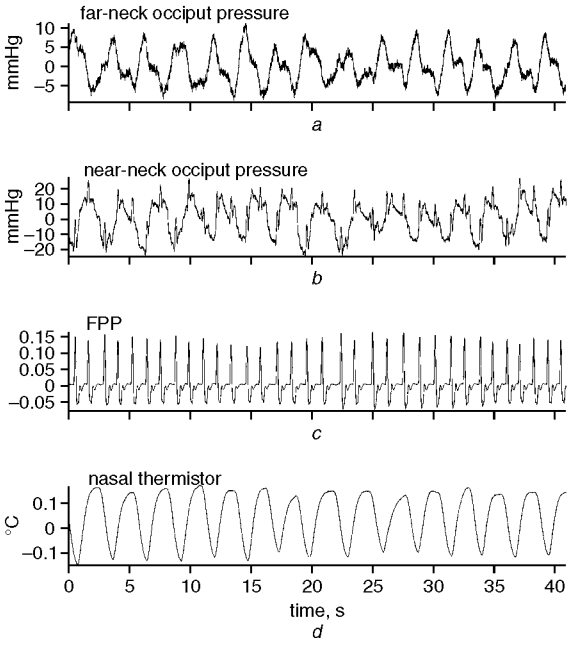

Fig. 2 *Four directly measured signals: (a) far-neck occiput pressure, (b) near-neck occiput pressure, (c) finger photo-electric plethysmogram (FPP) and (d) nasal thermistor signals. (a), (b) are pressure signals, and (c), (d) serve as reference data. Each is 40.96 s in length*

the digital signal ($x(n)$) can be calculated as follows:

$$A_{2^j}x(n) = \sum_{k\in Z} h_{0,2n-k} A_{2^{j-1}}x(k) \quad (2)$$

$$D_{2^j}x(n) = \sum_{k\in Z} h_{1,2n-k} A_{2^{j-1}}x(k) \quad (3)$$

where $A_{2^j}x(n)$ and $D_{2^j}x(n)$ are the approximation and detail components, respectively, in the 2^j scale, and $x(n)$ (or $A_{2^0}x(n)$) is the raw signal; h_0 and h_1 are the filter coefficients of $\boldsymbol{H}_0$ and $\boldsymbol{H}_1$, respectively. Therefore $A_{2^j}x(n)$ and $D_{2^j}x(n)$ ($j \in Z$) can be extracted from $x(n)$ (or $A_{2^0}x(n)$) using (2) and (3) recursively. The 2^{j-1} scale approximation signal can also be reconstructed from the 2^j scale approximation and detail components

$$\hat{A}_{2^{j-1}}x(n) = \sum_{k\in Z} g_{0,n-2k} A_{2^j}x(k) + \sum_{k\in Z} g_{1,n-2k} D_{2^j}x(k) \quad (4)$$

where g_0 and g_1 are the filter coefficients of $\boldsymbol{G}_0$ and $\boldsymbol{G}_1$, respectively. $\hat{x}(n)$ (or $\hat{A}_{2^0}x(n)$) can finally be reconstructed by repeatedly using (4). Noise in $D_{2^j}x(n)$ can be removed with the soft- or hard-threshold method before $\hat{A}_{2^{j-1}}x(n)$ is reconstructed. It should be pointed out that the sampling rate of the 2^j scale approximation and detail is just $f_s/2^j$, where f_s is the sampling rate of the raw signal.

Fig. 3 shows decomposed waveforms of the pulsatile pressure signal measured in the near-neckocciput. The raw signal shown in Fig. 3*a* is decomposed into $s = 2^j$, ($j = 1$–6) scales. Details from the 2^1–2^6 scales are shown sequentially in Figs 3*b*–*g*, and the 2^6 scale approximation is shown in Fig. 3*h*. The 2^6 scale approximation corresponds well to the respiration wave in the nasal thermistor signal (Fig. 2*d*), and the 2^4 and 2^5 scales' detail contain most of the signal energies and similar peaks to the pulse rate in the FPP. This implies that the 2^6 scale approximation (spectrum ranges from about 0 to 0.8 Hz) can be used to reconstruct the respiration rhythm, and the pulse rate can be synthesised from the 2^4 and 2^5 scales' detail (spectrum ranges from about 2 to 6 Hz) with the soft-threshold denoising method introduced in MALLAT and ZHONG (1992).

2.3 *Detection of pulse rate and respiration rhythm*

The respiration- or pulse-related waveform can be reconstructed from the 2^6 scale approximation or 2^4 and 2^5 scales'

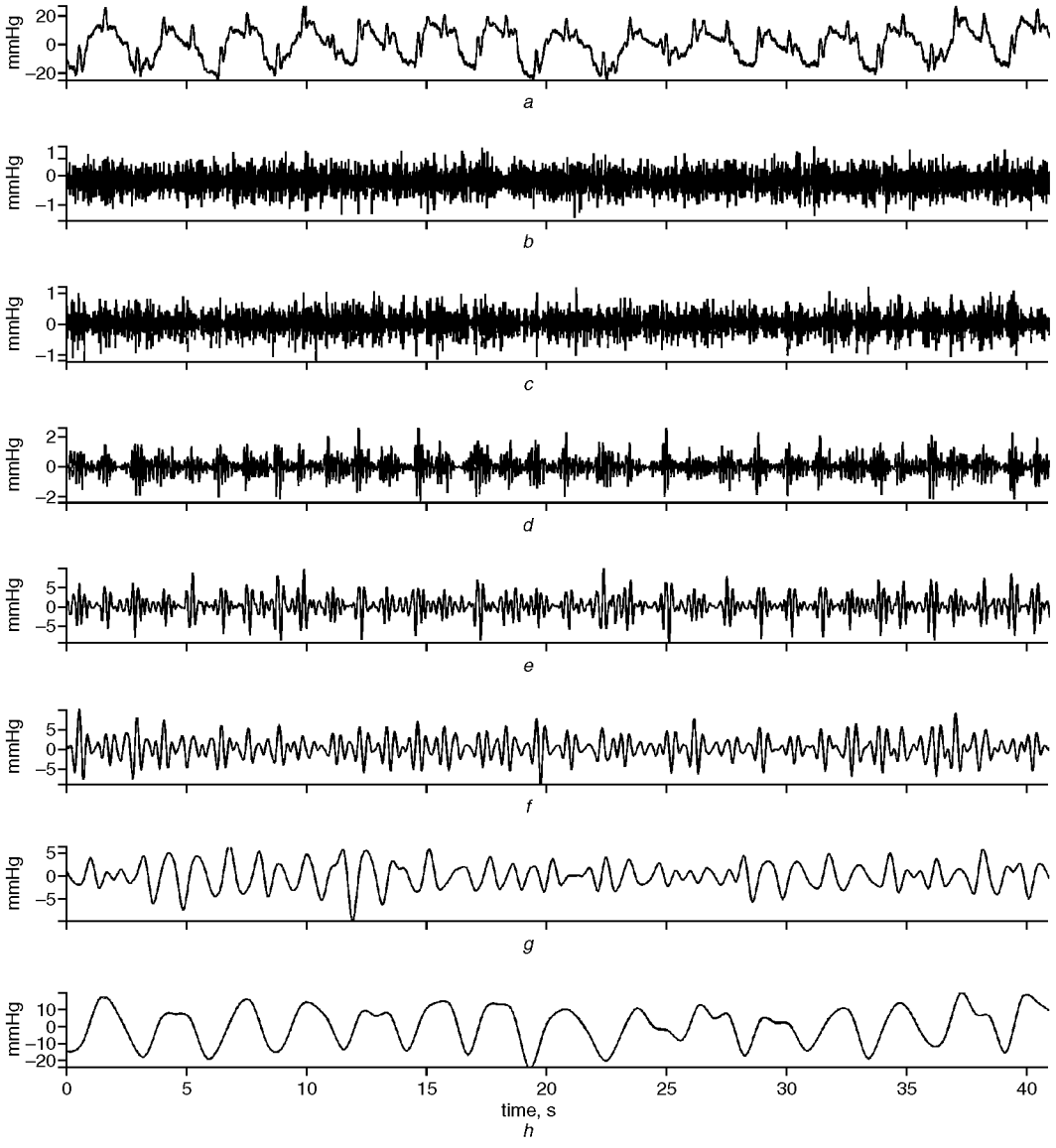

Fig. 3 *Wavelet decomposition of pressure signal from sensor in near-neck occiput region. (a) Raw signal (near-neck occiput pressure). (b)–(g) Waveforms reconstructed from detail components in 2^j ($j = 1$–6) scales, respectively. (h) Waveform reconstructed from approximation component in 2^6 scale*

details, respectively. The algorithm for detecting the pulse rate from the FPP and extracted pulse waveform is a refinement of the ECG peak search algorithms described in PAN and TOMPKINS (1985) and HAMILTON and TOMPKINS (1986). The characteristic point for pulse rate detection is defined as the peak with the highest amplitude and the largest slope in one heartbeat. To detect characteristic points from the FPP and extracted pulse-related waveform, both signals were first filtered through a first-derivative operator, and then points corresponding to the pulse peaks were determined by the zero-crossing point algorithm with a locally adaptive threshold. The characteristic point in the nasal thermistor signal and extracted respiration waveform is defined as the upward zero-crossing point, which corresponds to the middle of the exhaling process.

To avoid the influence of small amounts of noise, the zero line was locally adapted to compensate for the baseline drift, and only upward zero-crossing points with deep enough valleys ahead would be recognised as candidate points. Fig. 4*a* is the raw measured pressure signal in the near-neck occiput. Figs 4*b–e* show the FPP signal, extracted pulse wave, nasal thermistor signal and extracted respiration wave (their detected characteristic points are also marked with • in the Figure), respectively.

2.4 *Performance evaluation of detections*

Time shifts of detected points between reference and extracted signals can be found in Fig. 4. Time shifts between the FPP and extracted pulse in Figs 4*b* and *c* cannot be observed visually, whereas those between the nasal thermistor and extracted respiration in Figs 4*d* and *e* can be clearly identified. Because only the pulse rate and respiration rhythm every minute, other than the detected time of characteristic points in either reference or extracted signals, are concerned, a performance evaluation method for detection of the pulse rate and respiration rhythm is defined below.

(i) Count the number of detected peaks in the FPP and extracted pulse within each minute as *real pulse rate RPR* and *estimated pulse rate EPR*, respectively.

(ii) For each minute where *EPR* is higher than *RPR*, the *false positive number FPN* is defined as *EPR–RPR*. Summing all of the *FPN*s gives the *total false positive number TFPN*. Similarly, for each minute where *EPR* is lower than *RPR*, the *false negative number FNN* is given by *RPR–EPR*. Summing all of the *FNN*s gives the *total false negative number TFNN*.

(iii) The *false positive rate FPR* and *false negative rate FNR* are calculated as follows:

$$FPR = \frac{TFPN}{TRBN} \times 100(\%) \tag{5}$$

$$FNR = \frac{TFNN}{TRBN} \times 100(\%) \tag{6}$$

where *TRBN* denotes the total number of real heartbeats.

(iv) Similarly, count the number of detected upward zero-crossing points in the nasal thermistor and extracted respiration signal within each minute as the *real respiration rhythm RRR* and *estimated respiration rhythm ERR*, respectively.

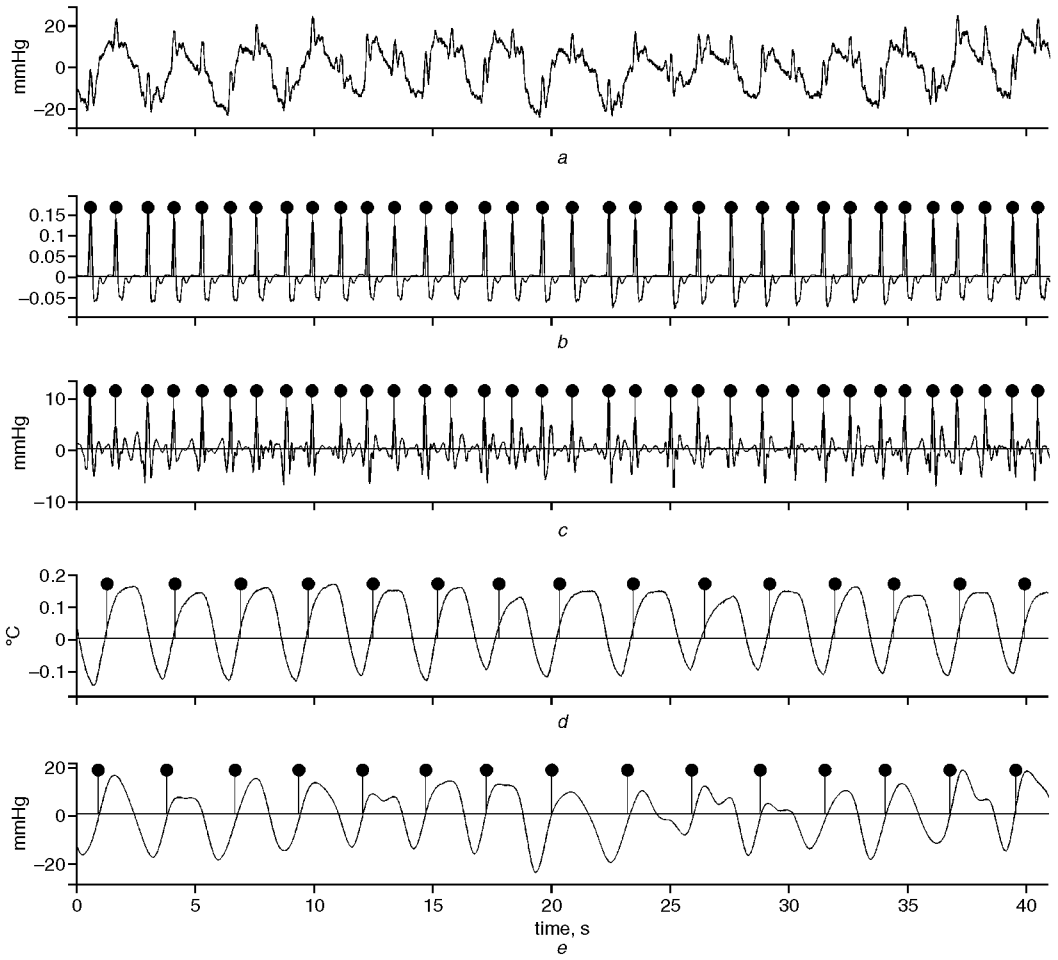

Fig. 4 *Two extracted signals corresponding to pulse and respiration rhythms, and detected characteristic points. (a) Raw signal. (b) FPP. (c) Extracted pulse rhythm. (d) Nasal thermistor signal. (e) Extracted respiration rhythm*

(v) For each minute where *ERR* is higher than the *RRR*, the *false positive number FPN* is defined as *ERR−RRR*. Summing all of the *FPN*s gives the total *false positive number TFPN*. Similarly, for each minute where *ERR* is lower than *RRR*, the *false negative number FNN* is given by *RRR−ERR*. Summing all of the *FNN*s gives the *total false negative number TFNN*.

(vi) As performance evaluation indexes for respiration rhythm, the *false positive rate FPR* and *false negative rate FNR* are given as follows:

$$FPR = \frac{TFPN}{TRRN} \times 100(\%) \quad (7)$$

$$FNR = \frac{TFNN}{TRRN} \times 100\% \quad (8)$$

where *TRRN* denotes the total number of real respirations.

2.5 *Subjects*

The near-neck occiput pressure data were collected from 13 healthy subjects (five female and eight male fourth-year students, from 21 to 22 years of age) at the School of Health Sciences, Kanazawa University, Japan. Approximately 2 h of data were acquired from each subject during sleep. As reference data for the pulse rate and respiration rhythm, the FPP and nasal thermistor signal were collected simultaneously.

3 Results

Fig. 5 shows a 64 min profile of estimation results and their errors: Fig. 5*a* shows *RPR* (marked ×) from the FPP and *EPR* (marked ○) from the extracted pulse waveform. Fig. 5*b* shows the relative estimation error percentage, derived by $(EPR-RPR)/RPR \times 100(\%)$. Similarly, *RRR* (marked ×) from the nasal thermistor and *ERR* (marked ○) from the extracted respiration waveform are shown in Fig. 5*c*. The relative estimation error percentage, derived by $(EPR - RRR)/RRR \times 100(\%)$, is shown in Fig. 5*d*. It can be reckoned that most relative estimation errors, for either the pulse rate or respiration rhythm, are within ±10%.

Pulse beat detection results from the FPP and extracted signal are tabulated in Table 1. The analysed data collected from 13 subjects were about 1500 min in length, and the total number of heartbeats counted was 91187 pulsations. The average value ± standard deviation for *FNR* and *FPR* were 3.03% ± 3.15% and 1.47% ± 0.63%, respectively.

Table 2 summarises the respiration detection results from the nasal thermistor and extracted signal. The analysed data were collected simultaneously with those in Table 1. The number of total respirations counted was 23 021 breathing movements. The average value ± standard deviation for *FNR* and *FPR* were 4.58% ± 3.23% and 3.07% ± 2.50%, respectively.

4 Discussion

WATANABE *et al.* (2003) proposed a digital filtering method to extract desired waveforms from the measured near-neck occiput pressure signal. A bandpass filter (0.1–0.8 Hz) gave the respiration-related signal, and the near-neck occiput pressure signal was directly regarded as the pulse-related signal. However, such a narrow, low-band filter requires a very high order to implement, and the respiration wave in the near-neck occiput pressure signal will influence the detection of the pulse rate. Moreover, the measurement noise and pulse-related signal sometimes overlap in the frequency domain. These would lead to failures in signal separation and would

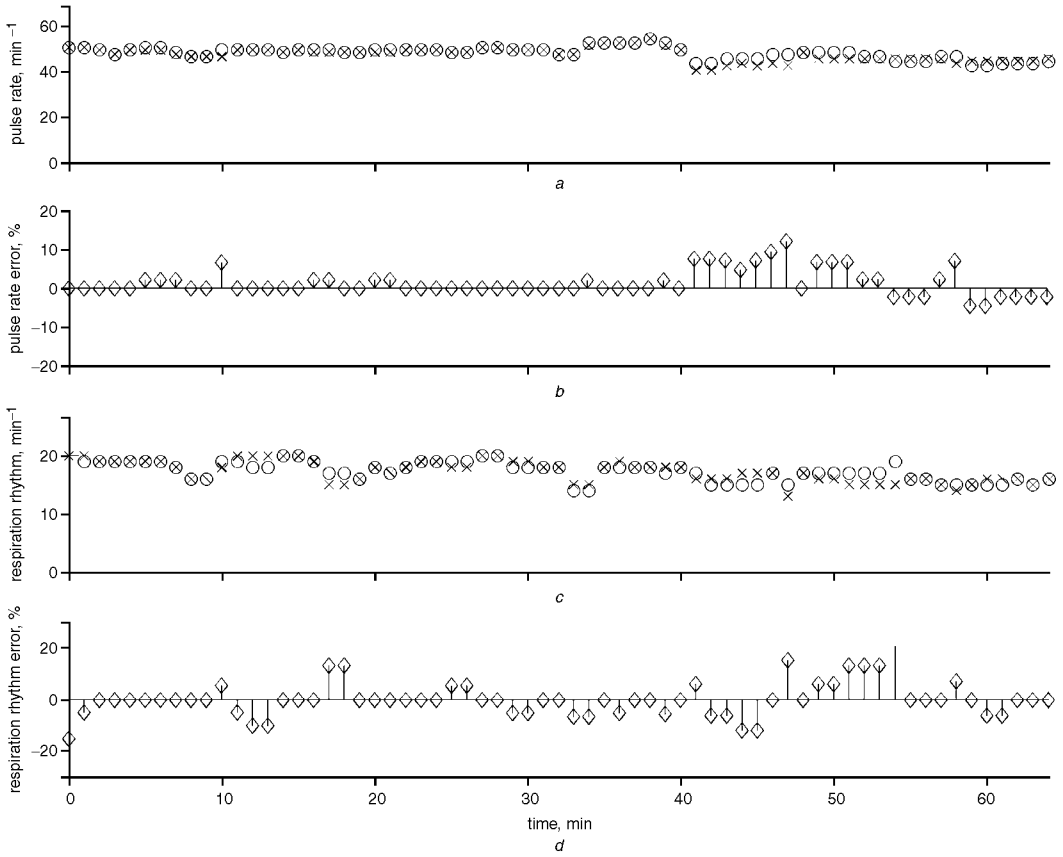

Fig. 5 *Instantaneous beat-by-beat profiles of (a) heart rate and (c) respiration rhythm detected from 10th subject (about 1 h of data) (×) results detected from reference data; ○ results from extracted signal) and beat-by-beat estimation errors of (b) heart rate and (d) respiration*

Table 1 Pulse beat detection results from FPP and reconstructed signal

Subject number	Data length, min	Number of heart beats detected by FPP signal	Number of heart beats detected by reconstructed signal	False rate, % negative	False rate, % positive
1	131.7	7891	7707	4.14	1.82
2	133.4	9081	8875	2.80	0.53
3	66.7	4747	4636	2.86	0.53
4	48.3	2919	2960	0.21	1.61
5	66.7	3723	3733	0.86	1.13
6	133.4	6681	6754	0.27	1.36
7	100.0	4708	4519	6.27	2.25
8	266.0	18029	17727	3.57	1.90
9	133.4	8680	8590	2.66	1.62
10	128.7	6014	6137	0.22	2.26
11	66.7	5242	4522	13.87	0.13
12	33.3	1870	1921	0.05	2.78
13	186.7	11602	11652	0.66	1.40
AVG	—	—	—	3.03*	1.47*
SD	—	—	—	3.15*	0.63*
Total	1495.0	91187	89733	—	—

*Weighted average, weighted by number of heart beats per case

FNR measures percentage of heartbeats undetected by algorithm while real beat exists, defined as $FNR = TFNN/TRBN \times 100(\%)$

FPR measures percentage of misdetected heartbeats by algorithm where no real beat exists, defined as $FPR = TFPN/TRBN \times 100(\%)$

Table 2 Respiration detection results from nasal thermistor and the reconstructed signal

Subject number	Data length, min	Number of respirations detected by thermistor signal	Number of respirations detected by reconstructed signal	False rate, % negative	False rate, % positive
1	131.7	1680	1791	4.05	10.65
2	133.4	2421	2376	2.35	0.50
3	66.7	1004	943	7.17	1.10
4	48.3	936	781	16.7	0.11
5	66.7	913	927	0.77	2.30
6	133.4	1881	1865	2.87	2.02
7	100.0	1341	1299	3.88	0.75
8	266.0	3924	3894	3.54	2.78
9	133.4	2127	2070	6.86	4.18
10	128.7	2244	2310	1.56	4.50
11	66.7	777	773	3.22	2.70
12	33.3	563	526	11.19	4.62
13	186.7	3210	3118	5.61	2.74
AVG	—	—	—	4.58*	3.07*
SD	—	—	—	3.23*	2.50*
Total	1495.0	23021	22673	—	—

*Weighted average, weighted by number of respiration cycles per case

increase the *false negative* or *positive rate* in the characteristic point detection. The spectral analysis method in KANEMITSU *et al.* (2004) cannot realise the beat-by-beat analysis and fails when the signal-to-noise ratio is too low.

It can be observed from Fig 2*a* and *b* that there exists a time lag between the far-neck occiput and near-neck occiput pressures. Because pressure variations, due to the breathing movement and pulsation, reach the two measurement sites (i.e. the far-neck occiput and the near-neck occiput) by two different transmission routes, this implies that a simple additive model is not accurate enough to describe the pressure variations in two occiput sites. The phenomenon leads to dissatisfaction with the instant mixing requirement in the linear ICA model (HYVÄRINEN, 1999) and therefore to incomplete separation of the pulse- and respiration-related signals (UCHIDA *et al.*, 2003).

Because the WT performs essentially as a bank of bandpass filters (LI *et al.*, 1995), this potential is successfully used to separate signals into different frequency components. It is well known that the fundamental frequencies of the respiration rhythm and pulse rate are located in different frequency bands. Through WT multiresolution decomposition and synthesis, the respiration- and pulse-related waveforms can be separated from each other in the measured pressure signal.

Furthermore, in contrast to the ICA method described in UCHIDA *et al.* (2003), the WT approach can extract the respiration- and pulse-related waveforms from only one channel's pressure signal. In addition, computational complexity can be greatly reduced, because only the corresponding components in characteristic scales need to be decomposed and reconstructed, unlike the time-consuming recursive optimisation calculation used in the ICA method.

The detection performance is evaluated using *FPR* and *FNR*. From Tables 1 and 2, it can be observed that *FNR* is higher than *FPR* in both the respiration rhythm and the pulse rate. This implies that most of the estimates tend to be lower in value than the reference data, and that few estimates have a higher respiration rhythm or pulse rate value than the reference data.

In Table 1, *FNR* in case 11 is much higher than that in the others. Because *FNR* measures the percentage of heartbeats undetected by the algorithm when a real beat exists, where real beats are measured by the FPP sensor with relatively less loss, the increase in undetected beats leads to the increase in *FNR* value. Two main possible reasons are considered responsible for the detection performance deterioration. One is the artifact induced by body movement. When a subject turns over in bed frequently during sleep, the measured pressure pattern distorts, and the characteristic points for the respiration rhythm and pulse rate cannot be properly detected from extracted signals. Another factor is sensor loss. When sensors are not well positioned beneath the pillow under the head, they fail to sense pressure variations. Then, neither the respiration- nor pulse-related signals can be reconstructed well.

Because only one channel of the pressure signal is used to extract the respiration rhythm and pulse rate, the measurement instrument configuration is greatly simplified. However, to improve detection performance, more robust algorithms and reliable detection strategies, as well as hardware designed to handle sensor loss and movement artifacts, would be helpful.

Future research should be conducted to enhance the real-time detection algorithm to meet practical needs. At the same time, clinical data regarding various sleep disorders should be collected and assessed so that the accuracy and reliability of this system as a sleep disorder monitor can be evaluated.

5 Conclusions

In this paper, a method to estimate respiration rhythm and pulse rate from the near-neck occiput pressure signal, which is completely non-invasive and unconstrained, being measured during sleep, was proposed and verified. The pressure signal is decomposed into detail and approximation components with the WT multiresolution analysis method. The respiration rhythm can be detected by the waveform reconstructed from the 2^6 scale approximation component, and the pulse rate can be obtained from the 2^4 and 2^5 scale detail components after noise depression with the soft threshold method. This

method provides a reliable and simple means to monitor for sleep apnoea and sudden death syndrome during sleep. Further, combining EEG and the present method will provide a powerful and convenient approach to search for the relationships between EEG, sleep stage, respiration rate and pulse rate.

Acknowledgments—The authors are grateful to the students at the School of Health Sciences, Kanazawa University, for their efforts in data collection.

References

AKAY, M. (1998): 'Time frequency and wavelets in biomedical signal processing' (IEEE Press, Piscataway, US, 1998), pp. 211–240

DAUBECHIES, I. (1992): 'Ten lectures on wavelets', in CBMS-NSF regional conference series in applied mathematics, vol. **61**, (Capital City Press, Montpelier, US, 1992), pp. 194–202

HAMILTON, P. S., and TOMPKINS, W. J. (1986): 'Quantitative investigation of QRS complex power spectra for design of a QRS filter', *IEEE Trans. Biomed. Eng.*, **33**, pp. 1157–1187

HILTON, M. L. (1997): 'Wavelet and wavelet packet compression of electrocardiograms', *IEEE Trans. Biomed. Eng.*, **44**, pp. 394–402

HYVÄRINEN, A. (1999): 'Fast and robust fixed-point algorithms for independent component analysis', *IEEE Trans. Newal Netro.*, **10**, pp. 626–634

KANEMITSU, Y., YAMASHITA, Y., NEMOTO, T., TAKADA, S., KITAMURA, K., YAMAKOSHI K., and CHEN, W. (2004): 'Development of biometry system in the sleep'. Proc. 43rd Ann. Conf. Jpn. Soc. ME & Biol. Eng., Kanazawa, Japan

KHAMENE, A., and NEGAHDARIPOUR, S. (2000): 'A new method for the extraction of fetal ECG from the composite abdominal signals', *IEEE Trans. Biomed. Eng.*, **47**, pp. 507–516

LI, C., ZHENG, C., and TAI, C. (1995): 'Detection of ECG characteristic points using wavelet transformation', *IEEE Trans. Biomed. Eng.*, **42**, pp. 21–28

MALLAT, S. (1989): 'A theory for multiresolution signal decomposition: the wavelet representation', *IEEE Trans. Pattern Anal. Mach. Intell.*, **11**, pp. 674–693

MALLAT, S., and HWANG, W. L. (1992): 'Singularity detection and processing with wavelets', *IEEE Trans. Inf. Theory*, **38**, pp. 617–643

MALLAT, S., and ZHONG S. (1992): 'Characterization of signals from multi-scale edges', *IEEE Trans Pattern Anal. Mach. Intell.*, **14**, pp. 710–732

MOODY, G. B., MARK, R. G., ZOCCOLA, A., and MANTERO, S. (1985): 'Derivation of respiratory signals from multi-lead ECGs', *IEEE Trans. Comput. Cardior.*, **12**, pp. 113–116

NAKAJIMA, K., YAMAKOSE, H., KUNO, H., NAMBU, M., IRIE, T., HIGUCHI, M., SAHASHI, A., and TAMURA, T. (2001): 'A pillow-shaped respiration monitor', *Life Support*, **13**, pp. 2–7

NAKAJIMA, K., YAMAKOSE, H., KUNO, H., NAMBU, M., IRIE, T., HIGUCHI, M., SAHASHI, A., and TAMURA, T. (2002): 'Evaluation for sleep apnea syndrome by a pillow-shaped respiration monitor', *Life Support*, **14**, pp. 14–19

PAN, J., and TOMPKINS, W. J. (1985): 'A real-time QRS detection algorithm', *IEEE Trans. Biomed. Eng.*, **32**, pp. 230–236

SHENSA, M. (1992): 'The discrete wavelet transformation, wedding the á trous and the Mallat algorithm', *IEEE Trans. Signal Process.*, **40**, pp. 2464–2484

TASWELL, C. (2000): 'The what, how, and why of wavelet shrinkage denoising', *IEEE Mag. Comput. Sci. Eng.*, May/June, pp. 12–19

UCHIDA, M., DING, S., CHEN, W., NEMOTO, T., and WEI, D. (2003): 'An approach for extractions of pulse and respiration information from pulsatile pressure signals'. Proc. IEEE Asia-Pacific BME Conf., Kyoto, Japan, CD-ROM

WATANABE, K., TASAKI, T., NEMOTO, T., YAMAKOSHI, K., and CHEN, W. (2003): 'Development of biometry system in the sleep by pillow cuff installed on the occiput', *Jpn. Soc. ME&BE Trans.*, **41**, p. 168

Authors' biographies

WENXI CHEN received BEng and MEng degrees both in Biomedical Engineering from Zhejiang University, China in 1983 and 1986 respectively. He obtained PhD in Medical Science from Tokyo Medical and Dental University in 2001. From 1992 to 1997, He had worked at R&D center, Nihon Kohden Corporation, Japan. He is currently an assistant professor at the Department of Computer Software, the University of Aizu, Japan. His research interests include biomedical instrumentation, non-invasive and ambulatory measurement of cardiovascular parameters, and related technologies toward ubiquitous healthcare application.

XIN ZHU is a doctoral student of the University of Aizu, Japan. He obtained his BS and MS degrees in Biomedical Engineering from Tianjin University, China in 2000 and 2002 respectively. His research interests are biomedical signal processing, modeling and simulation, and healthcare technology.

TETSU NEMOTO received a BS degree in Electronic Engineering from Nihon University, Japan in 1969. He obtained a PhD in Medical Science from Tokyo Medical and Dental University in 1984. From 1970 to 1987, he had worked as a technical official at Tokyo Medical and Dental University. From 1987 to 1992, he had worked as a chief researcher at National Institute of Animal Industry. From 1992 to 1999, he had worked as a head researcher at National Institute of Animal Industry. He is currently a professor in the Department of Laboratory Sciences School of Health science, Faculty of Medicine at the University of Kanazawa, Japan. His research interests include biomedical instrumentation, non-invasive and ambulatory measurement system of health care.

YUMI KANEMITSU graduated from Kansai University in 1991. She is working for SRI R&D Ltd. and developing a non-invasive system to measure heart rate and breathing rate during sleeping.

KEI-ICHIRO KITAMURA obtained a PhD in science from Kanazawa University Graduate School of Natural Science & Technology in 2002. From 1981 to 1996, he had worked at central laboratory of Kanazawa University hospital. He is currently an associate professor at the Department of Physical Information, School of Health Sciences, Faculty of Medicine, Kanazawa University. His research interests are non-invasive medical measurements of human and bone healthcare sciences.

KEN-ICHI YAMAKOSHI received the D.Med. and D.Eng. degrees from Tokyo Medical and Dental University, in 1979, and Waseda University, Tokyo, Japan, in 1982, respectively. He was a Research Assistant at Tokyo Women's Medical College from 1972 to 1973, a Research Assistant at Tokyo Medical and Dental University from 1974 to 1980, an Associate Professor at Hokkaido University, Sapporo, Japan, from 1980 to 1994, and has been a Professor at Kanazawa University, Kanazawa, Japan, since 1994. He is also currently a Visiting Professor at Dalian University, Dalian, China, and at Waseda University. His current research interests include non-invasive physiological measurements and instrumentation, health care monitoring, human support systems, biomechanics and rehabilitation engineering.